^{152}Eu DEPTH PROFILE OF STONE BRIDGE PILLAR EXPOSED TO THE HIROSHIMA ATOMIC BOMB

DATA ACQUISITION OF ^{152}Eu ACTIVITIES FOR THE ANALYSIS OF FAST NEUTRONS

Hiromi Hasai, Kazuo Iwatani, Kiyoshi Shizuma, Masaharu Hoshi, Kenjiro Yokoro, and Shozo Sawada
Hiroshima University

Toshiso Kosako
University of Tokyo

Yashige Morishima
Kinki University

The atomic bomb was detonated 580 m above Hiroshima City at 0815 hours on 6 August 1945. Later more than 100,000 survivors were selected and A-bomb doses, termed tentative 1957 dose (T57D) and tentative 1965 dose (T65D),[1] were determined for each survivor at the Atomic Bomb Casualty Commission (ABCC), later to become the Radiation Effects Research Foundation (RERF). The epidemiological studies performed at ABCC and RERF have been among the most important for evaluating risks due to radiation exposure.

In 1981, Marshall[2,3] described the results of Loewe's studies, which revealed discrepancies between the T65D and calculated free-in-air kerma. According to Loewe, the neutron dose in Hiroshima 1000 m from the hypocenter was about one-tenth that of T65D. The incidence of leukemia in Hiroshima was higher than that in Nagasaki according to an epidemiological study[4] using the T65D dose estimates. To explain this difference, Rossi and Mays[4] estimated the relative biological effectiveness (RBE) of neutrons as greater than one. If the neutron dose is actually very small, these discussions concerning derivations of neutron RBE must be greatly altered. Loewe determined the tissue kerma in air from computer

calculations. The main purpose of this paper is to verify the neutron dose using exposed materials in Hiroshima.

Among the many radioactivities induced by neutrons, data concerning the activities of ^{32}P, ^{152}Eu, ^{154}Eu, and ^{60}Co are available for neutron dose evaluations. Due to the short half-life of ^{32}P (14.2 days), its activity is not measureable now. The early measurement of sulfur in electric wire insulators by Yamasaki and Sugimoto[5] can only be used for evaluating high-energy neutrons (>3 MeV). However, errors in these data are relatively large and quantitative estimates of the efficiencies of the old detectors used are not easy. Data for ^{60}Co were obtained by Hashizume et al[6] using iron rings on rooftops and iron rods embedded in concrete in Hiroshima and Nagasaki. However, there are significant discrepancies between the calculated values of Loewe and the measured values, especially for Hiroshima (see Chapter 5). It is not easy to resolve these discrepancies. The radioactivities that can still be measured with statistical significance are those of ^{152}Eu, ^{154}Eu, and ^{60}Co, whose half-lives are 13.2, 8.5, and 5.3 years, respectively. Europium activities were detected by Sakanoue et al[7] and Nakanishi et al[8] and measurements were continued by Sakanoue et al (Chapter 5 Appendix 7) and by Okajima et al [9] (Chapter 5 Appendix 6), Takeshita et al,[10] and Hoshi et al[11] (Chapter 5 Appendix 5).

The doses of neutrons per unit fluence with energies over 0.5 MeV, for human bodies, are 30 to 40 times higher than those for thermal neutrons.[12] The neutron spectrum of the A-bomb has components of energies more than 0.5 MeV, and these portions contribute much of the absorbed dose in human bodies. For this reason, fast neutron fluences at the ground surface must be known to estimate the neutron dose for the A-bomb survivors.

Fast neutrons incident on a granite pillar surface lose their energies by scattering in the pillar and become slow or thermal neutrons. Then these neutrons induce ^{152}Eu activities in the pillar granite. Therefore, the resultant activity produced by these neutrons in the pillar granite reflects the history of the incident neutrons (i.e., the activity distribution in massive material contains information concerning the energy spectrum of the A-bomb). As the best available material of sufficient size and simple shape, granite pillars of the Motoyasu bridge were selected. Stable europium concentration in the granite pillar was only about 1 ppm; however, the ^{152}Eu radioactivity was sufficient for determining the depth profile owing to the large thermal neutron absorption cross section and its moderate half-life.

Reported here are the specific radioactivities of ^{152}Eu and ^{154}Eu and their depth profiles in the granite pillar to evaluate the neutron spectrum of the A-bomb. The depth profile will prove valuable to verify the neutron spectrum in air that was calculated by several authors[13,14] (Chapter 3) based on the source term obtained by Whalen.[15] The discussion concerning the 1986 dosimetry system (DS86; Chapter 9) and the evaluation of the A-bomb dose will be continued in forthcoming work.

Materials and Methods

Figure 1a shows the location of the Motoyasu bridge and its relationship to the hypocenter and epicenter. This bridge has eight pillars as shown in Figure 1b. Core samples were obtained from the pillar marked by an arrow in the figure. The distance from the hypocenter to the pillar is 132 ± 18 m and from the epicenter to the pillar is 595 ± 18 m (Figure 1c). The east-west and north-south coordinates of the pillar on the US Army Service Map, series

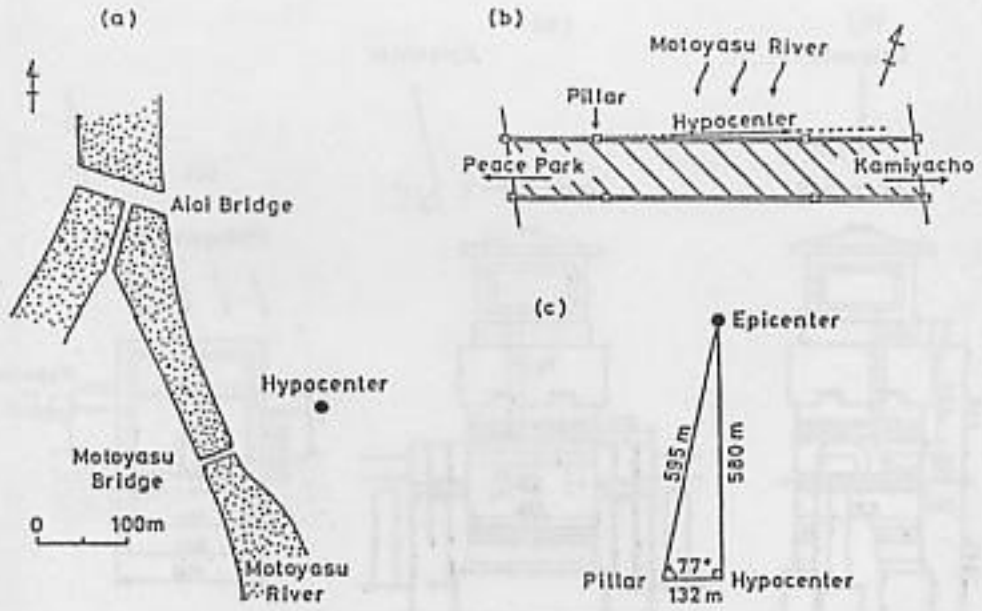

Figure 1. Location of Motoyasu bridge granite pillar. (a) Motoyasu bridge and the hypocenter. (b) Granite pillar from which the sample cores were obtained. (c) Bridge pillar and epicenter of the A-bomb

Table 1. Weather Conditions at the Time of the Hiroshima A-bomb

Weather	fine, clear
Air temperature	26.8 °C
Relative humidity	80 %
Air pressure	1018 mb
Moon phase	27.6 day

L902, plate number 138,499, are 744.16 and 1261.65. The hypocenter location was taken from Hubble.[16] Weather conditions at the time of the A-bomb are summarized in Table 1.

The shape of the pillar and the boring sites to obtain core samples are shown in Figure 2. There was a box and a roof (indicated by the dashed lines in Figure 2) on the top of this pillar to accomodate an electric light, and there was a vertical 3.5-cm diameter hole traversing the central part of the pillar to accomodate electric wires. Four 7.7-cm diameter cores were bored in the pillar as shown in Figure 2b. There were two horizontal cores along the directions from north to south (core 1) and from east to west (core 2) and a vertical core 75 cm long from the top of the pillar (core 3). Core 3 is composed of two parts, the upper portion 15 cm thick which was blown off at the time of the detonation and the lower 62 cm part. In addition to these samples, a concentric 12.7-cm diameter core (core 4) was bored in the same location as core 1 for analysis of elementary components. The height of core 1 from the river water surface was measured as 477 ± 8 cm at a tide level the same as that at the time of the detonation.

As shown in Figure 3, the core samples were cut into orbicular plates with an average thickness of 1.8 cm. The sample disks of cores 1 and 2 were labeled 1 to 41 from north to south and from west to east, respectively, and 1 to 37 from top to bottom for core 3. The

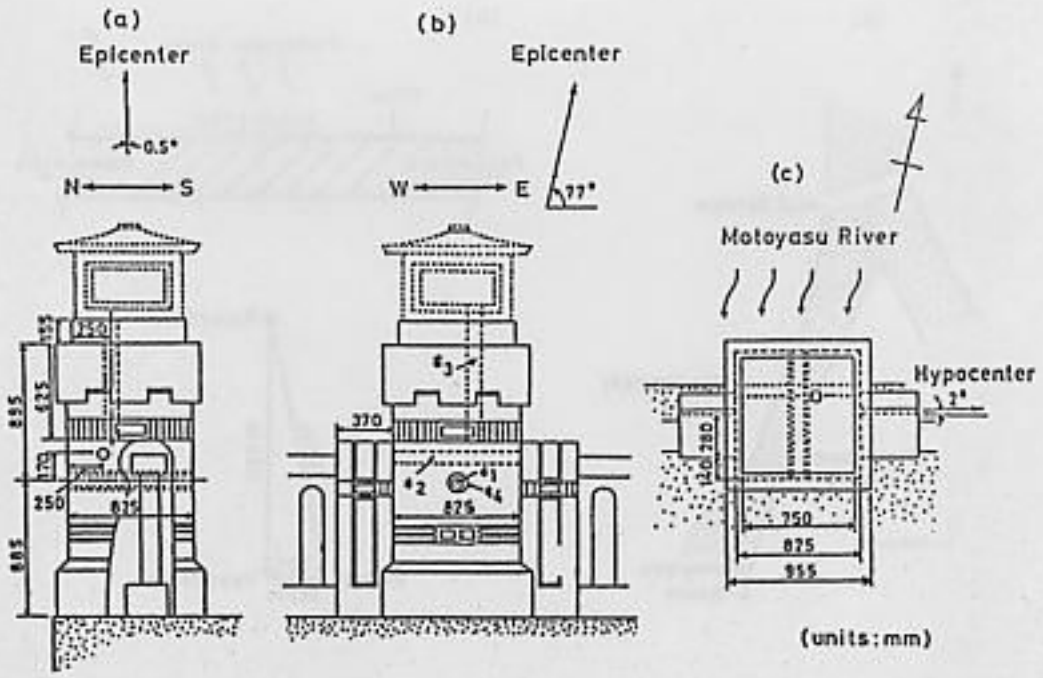

Figure 2. Detailed view of the granite pillar of the Motoyasu bridge and the boring sites of sample cores 1 to 4. View from (a) the west side, (b) the south side, and (c) top of pillar

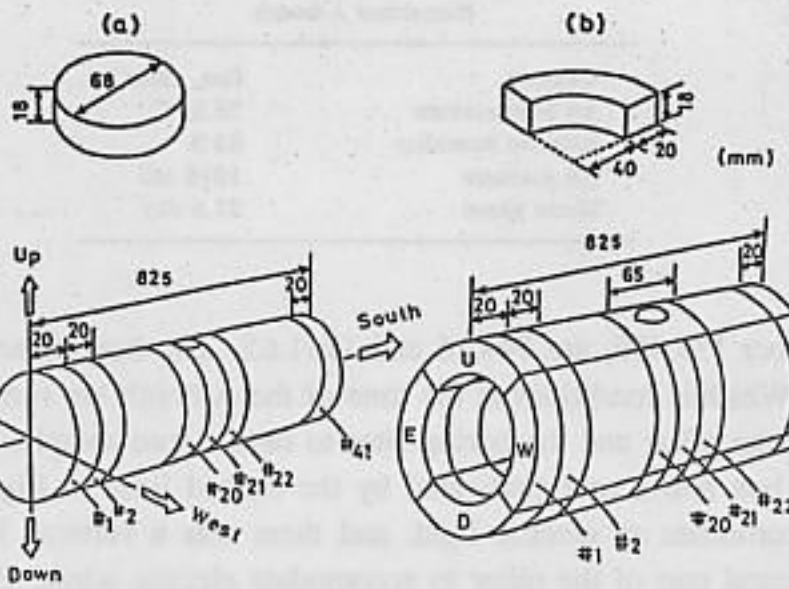

Figure 3. Schematic of sample cores 1 and 4

concentric core 4 was cut into four pieces from north to south and sectioned every 2 cm. All samples were marked N-MS, where N is the core number, M is the disk number, and S indicates direction such as E (east), W (west), N (north), S (south), U (up), and D (down).

Measurement and Results

Detector and Sample. A 124 cm^3 pure Ge detector (EG & G ORTEC) with a relative efficiency of 28% and an energy resolution of 1.74 keV (full-width at half maximum) at 1.33 MeV was used for the gamma-ray measurements. To measure the very low level ^{152}Eu

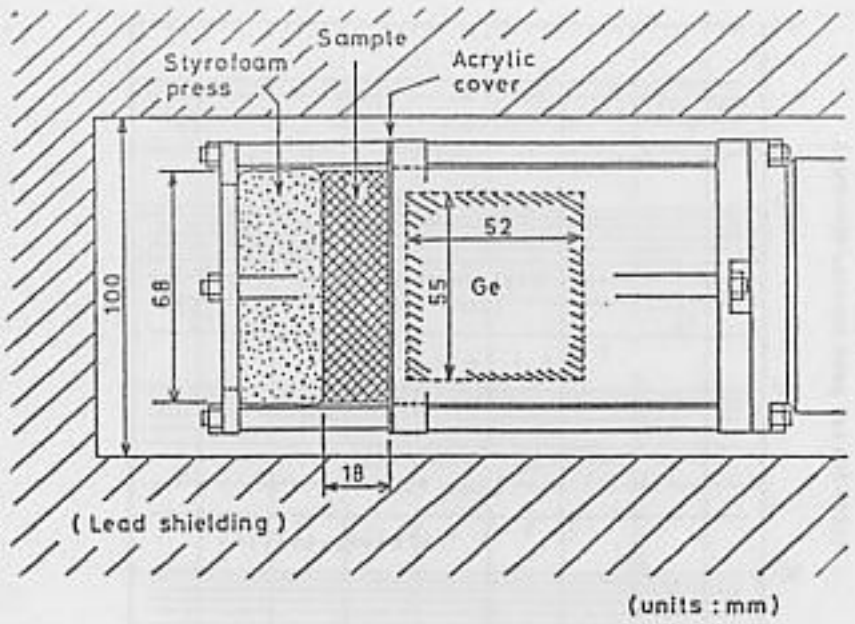

Figure 4. Measurement of a sample disk with a Ge detector with low-background lead shielding

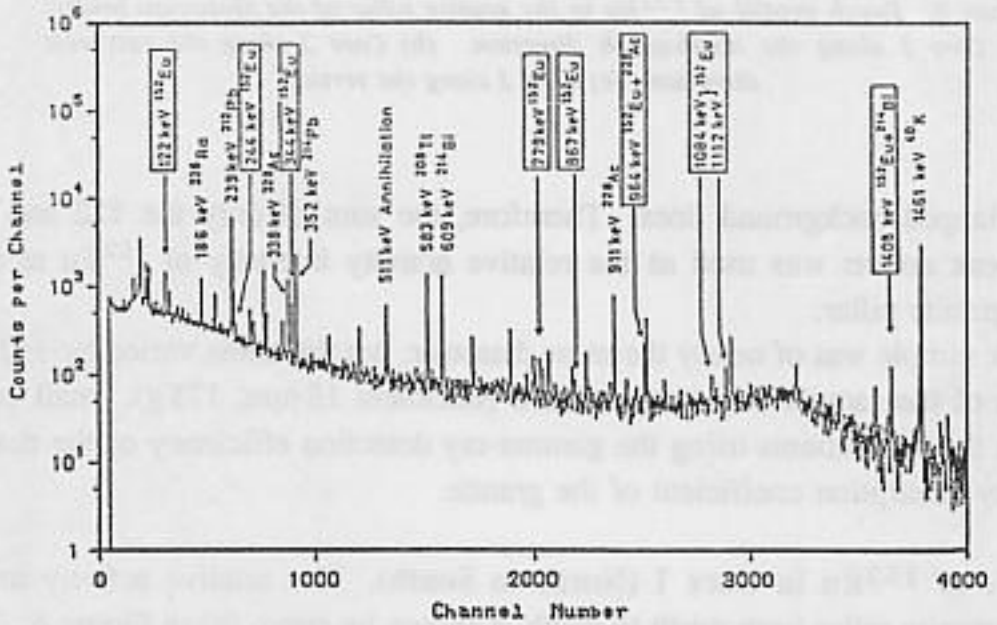

Figure 5. Typical gamma-ray spectrum of a sample disk (1-1N) from the Motoyasu bridge pillar. Gamma rays of ^{152}Eu are marked by arrows

activity in the sample, all gamma-ray measurements were performed with a low background shield composed of 20 cm thick lead blocks. The granite sample was placed close to the end cap of the detector, which was covered with a 1 mm thick acrylic plate, as shown in Figure 4.

Gamma rays were measured for one day. The sample was then turned end for end and measurements were continued during a second day. The average of the counts in the peak from both sides was taken as the gamma-ray peak count at the depth of the disk. Results for the spectrum of sample 1-1N are shown in Figure 5. Nine gamma rays from ^{152}Eu were observed in the spectrum. However, most line intensities were weak and some of their

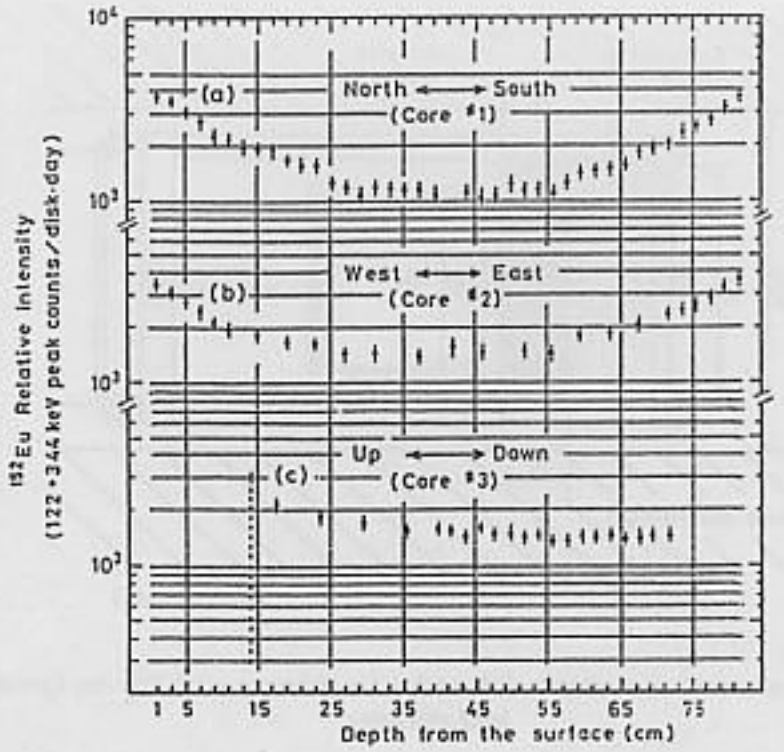

Figure 6. Depth profile of ^{152}Eu in the granite pillar of the Motoyasu bridge. (a) Core 1 along the north-south direction. (b) Core 2 along the east-west direction. (c) Core 3 along the vertical

energies overlapped background lines. Therefore, the sum of only the 122 and 344 keV gamma-ray peak counts was used as the relative activity intensity of ^{152}Eu at a specific depth in the granite pillar.

Every disk sample was of nearly the same diameter, but thickness varied by ± 2 mm. For normalization of the sample size to a standard (thickness 18 mm, 175 g), small corrections were made in the peak counts using the gamma-ray detection efficiency of the detector and the gamma-ray absorption coefficient of the granite.

Depth Profile of ^{152}Eu in Core 1 (North to South). The relative activity intensity of ^{152}Eu in the granite pillar from north to south is shown by curve (a) in Figure 6. The depth was measured from the north surface of the core. The intensities of ^{152}Eu activity were nearly the same at both the north and south surfaces, and it decreased to about 1/3.5 of the surface intensity at the center of the pillar. The distribution shows a nearly symmetric pattern. The error at each point includes the statistical error (i.e., the square root of the peak counts), and the uncertainty associated with the uniformity of stable europium distribution in the sample. The latter was estimated to have been about 6% of the peak counts.

Depth Profile of ^{152}Eu in Core 2 (West to East). The depth profile of ^{152}Eu activity in a west to east direction is of special interest, because the east side of the pillar directly faced the epicenter; whereas, its west side does not. Of the 41 disk-like samples of core 2, 25 samples were measured. Their depth profile is shown by curve (b) in Figure 6. The depth was measured from the western surface of the core. The results show no differences

between the eastern and the western surfaces of the pillar. Since the depth from the northern surface to this core was 25 cm, the distribution at depths between 25 and 65 cm became flat due to the dominant effect of the northern surface.

Depth Profile of ^{152}Eu in Core 3 (Vertical). The depth profile of the ^{152}Eu activity in a vertical direction is shown in curve (c) in Figure 6. The data for disks 1 to 7 obtained from the top plate (155 cm thick) are not shown in the figure since this plate was blown off at the time of the detonation. The ^{152}Eu activity became nearly constant at depths of more than 30 cm. At these depths, neutrons incident on the upper surface were sufficiently attenuated that neutrons from the northern and the southern surfaces became dominant, since the depth from these surfaces to core 3 was 25 cm. The ^{152}Eu activity in the samples at depths between 39 and 42 cm was measured carefully to check the uniformity of the stable europium distribution in the granite as described in the following section.

Composition of the Granite Sample. Analysis of the chemical composition of the granite sample was performed by the Kawatetsu Techno-Research Co., Ltd. (K-TEC). Results are shown in Table 2, except for europium and water. Measurements of stable europium concentrations and estimations of water content of the granite pillar were performed with special care.

Table 2. Chemical Composition of the Motoyasu Bridge Granite Pillar Excluding Europium and Water

Component	Weight Fraction
Fe_2O	2.27 %
SiO_2	74.2
Al_2O_3	13.6
CaO	1.84
MgO	0.06
MnO	0.04
K_2O	3.58
Na_2O	3.92
S	0.001
TiO_2	0.20

Density: 2.64 g/cm^3

Uniformity of Stable Europium in Granite. In principle, it is necessary to determine the eurpoium concentrations in all samples for the measurement of depth profiles of ^{152}Eu. In the present work, the europium concentration of each sample was estimated as follows. First, neutron activation analysis of seven samples was performed using the University Training and Research Reactor at Kinki University (UTR-KINKI). Results are shown in Table 3. The europium concentrations ranged from 0.85 to 1.05 μg g^{-1}. Second, the ^{152}Eu activity was measured for samples from core 3 at depths from 39 to 73 cm, where the neutron flux was considered uniform; data points gave a standard deviation of 6% on the average. Considering these experimental results, the uncertainty of uniformity of stable europium distributions in

Table 3. Concentration of Stable Europium in Granite Cores

Core Number	Disk Number	Concentration (μg/g)
4	1E, 1W	0.87 ± 0.06
4	8E, 8W	0.93 ± 0.09
4	40E	1.03 ± 0.12
	40U	1.05 ± 0.08
	40W	0.88 ± 0.10
	40D	0.85 ± 0.10
1	21	0.96 ± 0.06

core samples was estimated to be 6%, which was included in the experimental error associated with the depth profile data.

Water Content of the Granite. The water content of the granite is also important, because the neutron scattering cross section for hydrogen atoms is large. Several experiments were performed to elucidate how granite retains water. It was shown that the water consists mainly of penetration water, adsorptive water (I), adsorptive water (II), and bound water.

The first constituent consists of water formed when a rock becomes wet from rain or dew. This water penetrates from the surface of the rock into inter- and intra-granular cracks by capillary action. It evaporates from the surface of the rock in air. Its content in rock and its depth dependence are affected by weather conditions.

The second constituent consists of water adsorbed by the granular texture and liberated when the texture is broken (e.g., when the rock is ground into a fine powder).

Table 4. Water Content of the Motoyasu Bridge Pillar Granite

Component	Water Content (%)	Method of Measurement[a]
Penetration water	0 (lower limit) 0.16 ± 0.01 (upper limit)	A
Adsorptive water (I)	0.18 ± 0.10	A,B
Adsorptive water (II) (H_2O^-)	0.13 ± 0.01	B
Bound water (H_2O^+)	0.20 ± 0.01	B
Total	0.51 ± 0.10 (lower limit) 0.67 ± 0.10 (upper limit)	

[a]A: Gravimetry B: Karl Fisher volumetric method

The third and fourth constituents are for rock powder and are denoted by "H_2O^-" and "H_2O^+", respectively, in geological research. The amount for each constituent was measured for several granite samples from the pillar. The data obtained from the samples agreed with each other within an acceptable error in measurement. The average amounts are listed in Table 4. The lower and upper limits for penetration water have been obtained by submerging and drying experiments. Consequently, the total water content at the time of the bomb was estimated as 0.51 ± 0.10 to 0.67 ± 0.10%. Details concerning this determination are described in a separate report (K. Iwatani, to be published).

Table 5. Nuclear Data for ^{152}Eu and ^{154}Eu Production

Stable Isotope (Abundance)	(n, γ) Product	Half-life	Cross Section for Thermal Neutrons	Main Gamma-ray Energy (Intensity per Decay)
^{151}Eu (47.9%)	^{152}Eu	13.2 ± 0.3 y	5800 ± 200 b	121.8 keV (28.8 %)
	^{152m1}Eu	9.30 ± 0.05 h	3200 ± 200 b	
	^{152m2}Eu	96 ± 1 m	4 ± 1 b	
^{153}Eu (52.1%)	^{154}Eu	8.5 ± 0.5 y	380 ± 30 b	123.1 keV (41.4 %)

Data from: Lederer, C. M. and Shirley, V. S., 1978. *Table of Isotopes.* New York: Wiley Interscience.

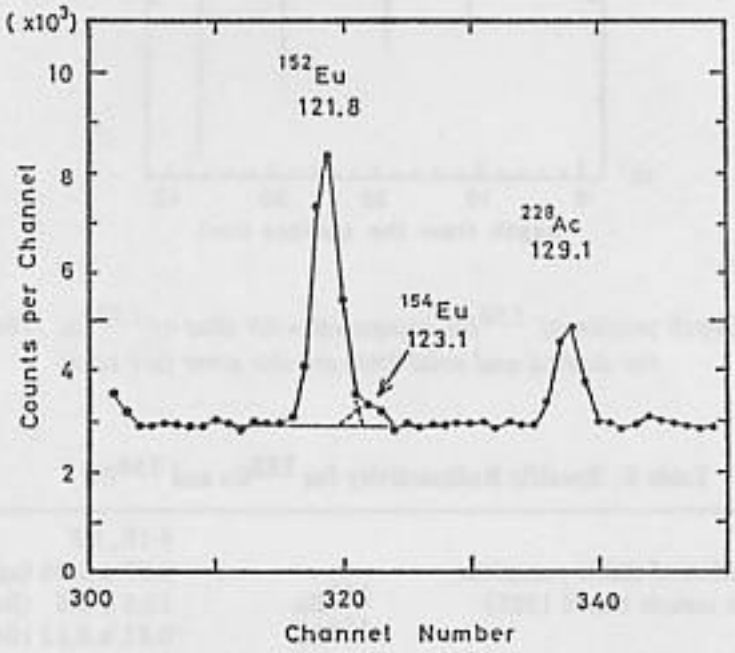

Figure 7. Example of a spectrum showing the ^{152}Eu 121.8 keV and the ^{154}Eu 123.1 keV doublet peaks

Observation of ^{154}Eu. Residual activity of ^{154}Eu that was produced by the neutron capture process, as well as ^{154}Eu, have been reported by Sakanoue et al[7,8] in the measurement of roof tiles and rocks exposed to the Hiroshima and Nagasaki A-bombs. The nuclear data for ^{152}Eu and ^{154}Eu activation are listed in Table 5. In the present work, the 123 keV line of ^{154}Eu was observed on the high energy side of the ^{152}Eu 122 keV line, and gamma rays with energies of 724 and 1,274 keV were also found with very low intensities by summing six spectra near the pillar surface. A typical spectrum is shown in Figure 7. Separating the 122 and 123 keV doublet by two-Gaussian fitting, a depth profile of the ^{154}Eu activity for core 1 was obtained as shown in Figure 8.

Specific Activities of ^{152}Eu and ^{154}Eu. To measure the absolute intensity of ^{152}Eu activity at the surface of the pillar, two northern surface samples, 4-1E,W (total 107 g) were ground into a fine powder (<100 mesh). Rock powder weighing 55 g was pressed into a

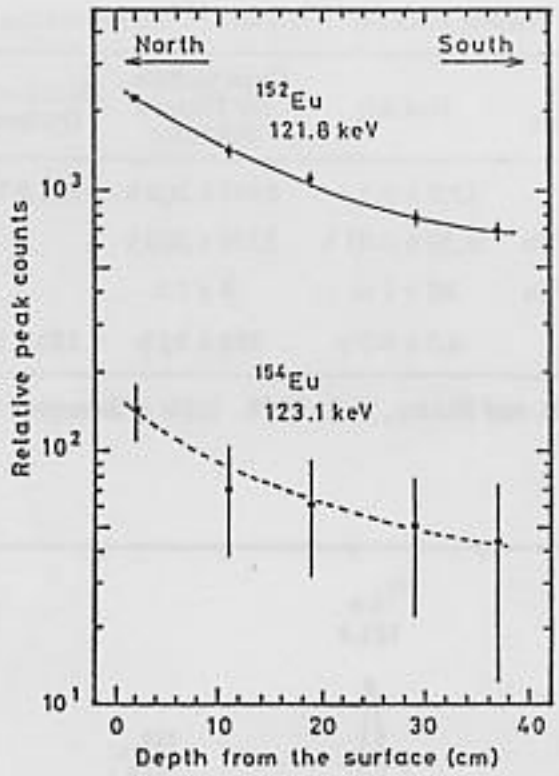

Figure 8. Depth profile of ^{154}Eu compared with that of ^{152}Eu. The slope of the dashed and solid lines are the same (see text)

Table 6. Specific Radioactivity for ^{152}Eu and ^{154}Eu

Sample		4-1E, 1W
Concentration of stable europium		0.87 ± 0.06 (μg/g)
Activity in sample (April 1985)	^{152}Eu	12.5 ± 0.6 (Bq/mg)
	^{154}Eu	0.81 ± 0.12 (Bq/mg)
Specific radioactivity[a]	^{152}Eu/Eu	117 ± 10 (Bq/mgEu)
	^{154}Eu/Eu	24 ± 4 (Bq/mgEu)

[a]Immediately after the detonation.

plastic container (60 mm diameter × 18 mm thick) and the ^{152}Eu intensity was measured. After a known amount of ^{152}Eu activity (4.47 Bq) was added to the powder sample and mixed well, the ^{152}Eu intensity was again measured. Thus, the ^{152}Eu activity in the sample was obtained as 0.0125 ± 0.0006 Bq g^{-1}. Using the stable europium concentration for this sample given in Table 3, the specific radioactivity ^{152}Eu/Eu immediately after the detonation was determined to be 117 ± 10 Bq mg^{-1}. The specific activity of ^{154}Eu and ^{152}Eu/Eu was also obtained as 24 ± 4 Bq mg^{-1}. These results are summarized in Table 6.

Discussion

Since the neutron absorption cross section for the ^{151}Eu(n,γ) ^{152}Eu reaction is large only in the energy region for slow neutrons (thermal, epithermal, and resonance regions), the depth profile of ^{152}Eu reflects fluences of slow neutrons directly, and fast neutrons indirectly, because they lose energy while slowing down in the granite. In the following

discussion, specific radioactivities for ^{152}Eu and ^{154}Eu at the granite surface were compared with recent calculations of neutron fluences, and the ^{152}Eu depth profile data were compared with calculations assuming only thermal neutrons incident.

Specific Activity for ^{152}Eu and ^{154}Eu at the Pillar Surface. Pace,[14] of Oak Ridge National Laboratory (ORNL), calculated the neutron fluence 1 m above ground level for the Hiroshima bomb, per kiloton of explosive yield, in 37 energy groups for ranges between 9.38 m and 2,000 m from the hypocenter. Neutron fluence was also calculated by Loewe[13]; a complete discussion of the neutron calculations is given in Chapter 3. Based on these neutron fluences, specific radioactivities for ^{152}Eu (S_1) and ^{152}Eu (S_2) can be calculated by the following equations.

$$S_1 = \frac{Y_1 A \lambda_1}{M 10^3} (\phi_1 \sigma_1 + \phi_2 \sigma_2 \cdots), \; Bq\, mg^{-1}\, (of\ Eu) \tag{1}$$

$$S_2 = \frac{Y_2 A \lambda_2}{M 10^3} (\phi_1 \sigma_1^{\dagger} + \phi_2 \sigma_2^{\dagger} \cdots), \; Bq\, mg^{-1}\, (of\ Eu) \tag{2}$$

where Y_1 and Y_2 are the natural isotopic abundances for ^{151}Eu and ^{153}Eu, A is the Avogadro number, M is the average atomic mass of europium, λ_1 and λ_2 are the decay constants of ^{152}Eu and ^{154}Eu, ϕ_i is the neutron fluence of the i-th energy group, σ_i and $\sigma_i^{\dagger}$ are average cross sections of the (n.γ) reaction in the neutron energy region of the i-th group for ^{152}Eu and ^{154}Eu, respectively.

S_1 and S_2 were calculated using the ORNL fluence assuming the explosion yield to be 15 kt and the Japanese evaluated nuclear data library[17] for neutron activation cross sections. The cross sections in the resonance region were smoothed by using experimental values given in a Brookhaven National Laboratory report.[18] In Figure 9, experimental values obtained in the present work and the former measurements by Nakanishi et al[8] (open circles) are given as a function of distance from the epicenter. The present experimental value agrees well with those of Nakanishi et al[8] for ^{152}Eu. The dashed lines in Figure 9 represent our calculated values based on the ORNL neutron fluence. It should be noted that only the neutron fluence in air was used in the calculation and neutron scattering by surrounding material such as pillar granite was not included. If one considers such a scattering effect, the yields of ^{152}Eu and ^{154}Eu become higher by about 10% or more. In addition, thermal neutron fluence varies from place to place because of differences in the surroundings from which the samples were taken. So, data obtained from among surface materials sometimes differ, with wide discrepancies. The solid line in the figure represents calculations by Loewe[19] for ^{152}Eu. The former curve is somewhat higher than the latter near the hypocenter. In the case of ^{152}Eu, experimental values agree with Loewe's calculation within 20%.

Depth Profile of ^{152}Eu. In this section, a simple estimate for the depth profile of ^{152}Eu is presented assuming only thermal neutrons incident to estimate the fast neutron contribution to the profile.

Macroscopic cross sections for absorption (Σ_a) and scattering (Σ_s) of thermal neutrons

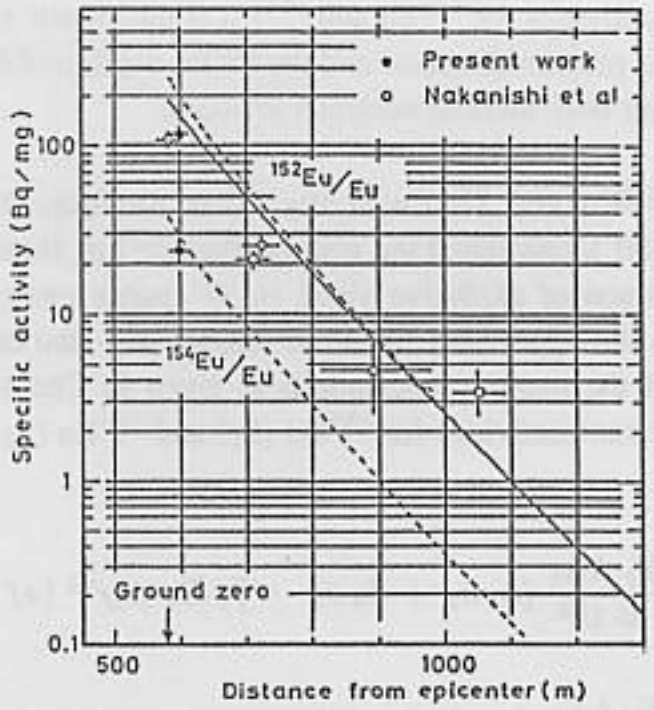

Figure 9. Specific radioactivity for ^{152}Eu and ^{154}Eu as a function of distance from the epicenter. The black dots represent data obtained in the present study; the open circles represent data of Nakanishi et al.[8] The dashed lines represent calculations based on ORNL neutron fluences; the solid line for ^{152}Eu represent calculations of Loewe.[19]

by an element in granite can be represented as follows,

$$\Sigma_a \text{ or } \Sigma_s = \frac{\rho A \omega \sigma_a \text{ or } \sigma_s}{M}, \ cm^{-1} \tag{3}$$

where ρ is the density of the rock, A is the Avogadro number, ω is the weight fraction of the element, σ_a is the absorption cross section, σ_s is the scattering cross section, and M is the atomic mass of the element. The macroscopic cross sections were calculated for 12 elements contained in the granite and the results are given in Table 7. Then the diffusion length L is represented as

$$L = \frac{1}{\sqrt{\tilde{\Sigma}_a \tilde{\Sigma}_s}}, \ cm \tag{4}$$

where $\tilde{\Sigma}_a$ and $\tilde{\Sigma}_s$ are summations of Σ_a and Σ_s for 12 elements. A value of L = 10.1 cm was obtained for the granite.

As shown in Figure 6, the ^{152}Eu activity has nearly the same intensity at all side surfaces of the pillar. This fact indicates that neutron fluences were nearly the same at these pillar surfaces because the pillar was located nearly beneath the epicenter. Based on these facts and assuming that the thermal neutron fluence decreases as $e^{-x/L}$ in the granite, where x (cm) is depth in rock from the surface, the depth profile for the pillar can be simply represented as follows,

Table 7. Element Composition of the Motoyasu Bridge Granite Pillar and Macroscopic Cross Sections for Thermal Neutrons

Element	Atomic Concentration (10^{20} atom/cc)	Atomic Cross Section		Macroscopic Cross Section	
		σ_a (b)	σ_s (b)	Σ_a (cm^{-1})	Σ_s (cm^{-1})
H	10.4	0.33	81.5	3.5×10^{-4}	8.5×10^{-2}
O	490	0.00027	3.76	1.3×10^{-5}	1.8×10^{-1}
Na	20.1	0.53	3.2	1.1×10^{-3}	6.4×10^{-3}
Mg	0.24	0.064	3.4	1.5×10^{-6}	8.0×10^{-5}
Al	42.4	0.23	1.5	9.8×10^{-4}	6.3×10^{-3}
Si	196	0.17	2.2	3.2×10^{-3}	1.3×10^{-2}
K	12.1	2.1	1.5	2.5×10^{-3}	1.8×10^{-3}
Ca	5.2	0.43	3.2	2.2×10^{-4}	1.7×10^{-3}
Ti	0.40	6.1	4.0	2.4×10^{-4}	1.6×10^{-4}
Mn	0.087	13.3	2.1	1.2×10^{-4}	1.8×10^{-5}
Fe	4.53	2.6	10.9	1.2×10^{-3}	4.9×10^{-3}
Eu	9.1×10^{-5}	4511.0	8.0	4.1×10^{-5}	7.2×10^{-3}

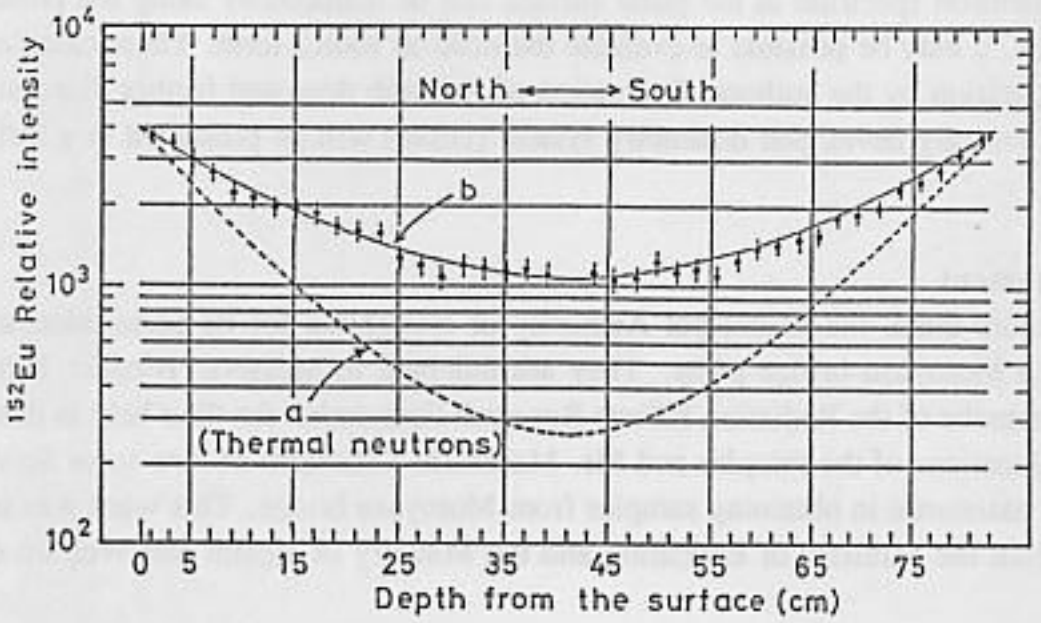

Figure 10. Comparison of the depth profile with a simple calculation. Curve (a) indicates a calculation assuming only thermal neutrons were incident and using a diffusion length L = 10.1 cm. Curve (b) indicates a best fitted calculation using effective diffusion length L = 16.5 cm (see text)*

$$I(x) = I_o\,(e^{-x/L} + e^{-(82-x)/L}) + 2C \qquad (5)$$

where $C = I_o\, e^{-41/L}$ is the contribution from the eastern or the western surfaces. The result is shown by curve (a) in Figure 10. A large discrepancy is clearly seen between the actual and the calculated depth profiles. This discrepancy can be attributed to the energetic neutrons included in the actual neutron spectrum. To fit the experimental points of the depth profile at the surface and the central part of the pillar, an "effective" diffusion length $L*$

= 16.5 cm was obtained, which is longer than L = 10.1 cm. The curve (b) in Figure 10 is obtained using $L*$ instead of L in Equation (5). As shown in Figure 2, there are two subpillars (height 1,155 cm, thickness 37 cm, width at the neck 28 cm) at the east and west side of the main pillar. If the subpillars caused "shadows" on the depth profile for core 1 (north-south), the ^{152}Eu activity intensity would be decreased at depths from 40 to 60 cm. This is probably related to the fact that the intensities at depths between 55 and 70 cm are about 8% lower than those at depths from 20 to 40 cm.

Summary

In order to verify the reliability of the neutron calculations (Chapter 3),[13,14,19] the ^{152}Eu depth profile of a granite pillar of the Hiroshima Motoyasu bridge offered fundamental experimental data. This report contains evidence that neutrons more energetic than thermal neutrons were present in the actual neutron spectrum. Further calculations including the neutron transport in rock using the Monte Carlo code will be needed to reproduce the ^{152}Eu depth profile in detail, reflecting the neutron spectrum of the A-bomb.

If the response function for ^{152}Eu production in rock for various neutron energies is obtained, the neutron spectrum at the pillar surface can be deduced by using the present depth profile. Then, it may be possible to evaluate the neutron source term. These calculations are now in preparation by the authors. Evaluation of A-bomb dose and further discussions concerning the recently developed dosimetry system (DS86) will be presented in a forthcoming report.

Acknowledgment

The authors thank the Municipal Authority of Hiroshima for its permission to sample cores from a Motoyasu bridge pillar. They are indebted to Messers. Hiroaki Yamada and Tadaaki Watanabe of the Radiation Effects Research Foundation for their help in determining the precise locations of the samples and Mr. Masatoshi Takahashi of Ken-setsu Service, Co., Inc., for his assistance in obtaining samples from Motoyasu bridge. This work was supported by grants from the Ministry of Education and the Ministry of Health and Welfare of Japan.

References

1. Milton, R. C. and Shohoji, T., 1968. Tentative 1965 Radiation Dose Estimation for Atomic Bomb Survivors. Hiroshima: Radiation Effects Research Foundation, ABCC report TR 1-68.
2. Marshall, E., 1981. New A-bomb studies after radiation estimates. Science 212:900-903.
3. Marshall, E., 1981. New A-bomb data shown to radiation experts. Science 212:1364-1365.
4. Rossi, H. H. and Mays, C. W., 1978. Leukemia risk from neutrons. Health Physics 34:353-360.
5. Yamasaki, F. and Sugimoto, A., 1953. Radioactive ^{32}P in sulfur in Hiroshima. In Collection of Investigative Reports on Atomic Bomb Disaster, Vol. I, pp. 16-18. Tokyo: Japanese Science Promotion Society.
6. Hashizume, T., Maruyama, T., Shiragai, A., Tanaka, E., Izawa, M., Kawamura, S., and Nagaoka, S., 1967. Estimation of the air dose from the atomic bombs in Hiroshima and Nagasaki. Health Physics 13:149-161.
7. Sakanoue, M., Maruo, Y., and Komura, K., 1981. In Int. Symp. Methods Low-Level Counting and Spectrometry, pp. 105-124. Vienna: International Atomic Energy Agency, publication STI/PUB/592.

8. Nakanishi, T., Morimoto, T., Komura, K., and Sakanoue, M., 1983. ^{152}Eu in samples exposed to the nuclear explosions at Hiroshima and Nagasaki. Nature 302:132-134.

9. Okajima, S. and Miyajima, J., 1983. Measurement of neutron-induced ^{152}Eu radioactivity in Nagasaki. In U.S.-Japan Joint Workshop for Reassessment of Atomic Bomb Radiation Dosimetry in Hiroshima and Nagasaki, pp. 156-168. Hiroshima: Radiation Effects Research Foundation.

10. Takeshita, K., Hoshi, M., Kato, K., Takeoka, S., Ogawa, M., and Tsuruta, T., 1982. Measurements of induced activites by Hiroshima A-bomb and the reevaluation of the A-bomb dose. Osaka: Kyoto University, paper presented at the 16th Symp. of the Research Reactor Institute.

11. Hoshi, M., 1982. Reevaluation of atomic bomb dose in Hiroshima and Nagasaki. In Annual Report of Research Institute for Nuclear Medicine and Biology, pp. 87-92. Hiroshima: Hiroshima University.

12. International Commission on Radiological Protection, 1971. Data for Protection Against Ionizing Radiation from Experimental Sources. Oxford: Pergamon Press, ICRU Publication 21.

13. Loewe, W. E., 1985. Initial radiations from tactical nuclear weapons. Nucl. Tech. 70:274-284.

14. Pace, J. V., 1983. ORNL neutron fluence by distance from the hypocenter for the Hiroshima bomb at one meter above the ground. In U.S.-Japan Joint Workshop for Reassessment of Atomic Bomb Radiation Dosimetry in Hiroshima and Nagasaki, pp. 218-224. Hiroshima: Radiation Effects Research Foundation.

15. Whalen, P. P., 1983. Source terms for the initial radiations. In U.S.-Japan Joint Workshop for Reassessment of Atomic Bomb Radiation Dosimetry in Hiroshima and Nagasaki, pp. 12-44. Hiroshima: Radiation Effects Research Foundation.

16. Hubbell, H. H., Jones, T. D., and Cheka, J. S., 1969. The Epicenters of the Atomic Bombs: Part 2. Reevaluations of All Available Physical Data with Recommended Values. Hiroshima: Radiation Effects Research Foundation, ABCC report TR 3-69.

17. 1984. Japanese Evaluated Nuclear Data Library, second version. Nuclear Data Center, JAERI.

18. Mughhabghab, S. F., and Garber P. I., 1973. Neutron Gross Sections, Vol. 1, BNL-325, Third Edition.

19. Loewe, W. E., 1986. Personal communication. Livermore, CA: Lawrence Livermore National Laboratory.